

Joint Estimation of DOA and Frequency with Sub-Nyquist Sampling in a Binary Array Radar System

Zhan Zhang*, Ping Wei*, Lijuan Deng*, Huaguo Zhang*†

*School of Information and Communication Engineering,
University of Electronic Science and Technology of China, Chengdu 611731, China

*Email: zzhenry15@163.com

†Science and Technology on Communication Information Security Control Laboratory,
Jiaxing, China

Abstract—Recently, several array radar structures combined with sub-Nyquist techniques and corresponding algorithms have been extensively studied. Carrier frequency and direction-of-arrival (DOA) estimations of multiple narrow-band signals received by array radars at the sub-Nyquist rates are considered in this paper. We propose a new sub-Nyquist array radar architecture (a binary array radar separately connected to a multi-coset structure with M branches) and an efficient joint estimation algorithm which can match frequencies up with corresponding DOAs. We further come up with a delay pattern augmenting method, by which the capability of the number of identifiable signals can increase from $M - 1$ to $Q - 1$ (Q is extended degrees of freedom). We further conclude that the minimum total sampling rate $2MB$ is sufficient to identify $K \leq Q - 1$ narrow-band signals of maximum bandwidth B inside. The effectiveness and performance of the estimation algorithm together with the augmenting method have been verified by simulations.

Index Terms—DOA estimation, frequency estimation, sub-Nyquist sampling, binary array radar

I. INTRODUCTION

In array radar signal processing, joint frequency and direction-of-arrival (DOA) estimation problems have received extensive attention. Modern signals have relatively high carrier frequencies and are distributed over a comparatively wide spectrum range. According to Nyquist Sampling [1], samplers will face high conversion speed problem and considerable data pressure, which facilitates the rapid development of sub-Nyquist sampling techniques [2]. Therefore, how array radars can jointly estimate frequencies and orientations of signals effectively at sub-Nyquist Sampling has been extensively studied.

In the literature, many methods such as [3], [4] have efficiently achieved joint estimations of DOAs and corresponding carrier frequencies at Nyquist sampling. However, these methods cannot work well at sub-Nyquist sampling. The approaches such as [5], [6] overcome this defect and can make joint estimation at sub-Nyquist sampling. Nevertheless, Zoltowski et al present [5] to decompose the entire spectrum into overlapping sub-band via such a structure (each antenna

followed by a filter bank and a mixer) and each band has to be examined separately by two paths (a direct path and a delayed path), which causes more hardware resources and quite slow processing speed. On the other hand, Ariananda et al [6] put forward to connect a multi-coset structure [7] to each antenna of the minimum redundancy linear array (MRA) [8] to implement joint estimation with sub-Nyquist sampling. This array arrangement also causes high consumption. Recently, Liu et al come up with [9], [10] to jointly estimate frequencies and DOAs with sub-Nyquist sampling for more sources than sensors. However, these methods also bring high hardware pressure; the total sampling rate, i.e., the sum of sampling rates for all channels, is fairly high even though the sampling rate of each channel is lower than the Nyquist sampling rate.

To overcome the problems of high hardware resource consumption and high total sampling rate, Kumar et al have suggested a simple sub-Nyquist sampling architecture [11], [12] together with the corresponding algorithm. This architecture is that each receiver has only two paths, a direct path and a delayed path, followed by an ADC separately. The corresponding algorithm is based on MUSIC algorithm [13] and ESPRIT algorithm [14], which can realize joint estimations of DOAs and frequencies at a fairly low total sampling rate. Due to the limitation of Kruskal rank [15], in order to avoid the blurring problem of frequency and DOA estimation, this algorithm cannot be applied the in uniform linear array (ULA), but in circular shape array [11] and rectangular nested array [12], which illustrates some certain limitations for the array layout. Moreover, based on the generalized eigendecomposition of the matrix beam, its frequency estimation is too sensitive to noise. Thus, a two-dimensional multiresolution algorithm has to be applied to solve performance problems.

The paper aims to to achieve joint estimations of frequencies and corresponding DOAs effectively at a very low total sampling rate in an array radar system, where the number of array elements is fewer than that of signals. We propose a binary array radar structure and corresponding joint estimation algorithm with high efficiency, which can automatically pair frequencies and DOAs to overcome the ambiguity problem

Identify applicable funding agency here. If none, delete this.

[11]. Moreover, an augmenting method similar to literature [10] is presented, which can be applied to estimate more signal parameters with fewer channels.

The paper is organized as follows: in the next section, we introduce the scenario together with signal model and present a binary array radar architecture. In section III, we describe our algorithm as well as an expansion of time-delay manifold method, and give the boundary of the minimal total sampling rate. Section IV shows simulation results and offers some further discussion. Finally, section V comes to the conclusion.

II. SIGNAL MODEL AND PROPOSED ARRAY STRUCTURE

In this section, we first describe the scenario including the signal model and some specific assumptions. Then a binary array radar structure is introduced, and corresponding array received signal model is given.

A. Signal Model

Consider such a scenario where K uncorrelated, narrow-band, far-field signals spreading over a very wide spectrum range from different orientations are received by a radar array. These K signals, considered as time domain wide multiband signals (MBS), i.e., many disjoint narrow-band signals within a wide-band spectrum, are denoted as $x(t)$ and can be expressed as

$$x(t) = \sum_{k=1}^K s_k(t) e^{j2\pi f_k t} \quad (1)$$

Then, the time delay expression of $x(t)$ with time difference τ can be written as

$$\begin{aligned} x(t-\tau) &= \sum_{k=1}^K s_k(t-\tau) e^{j2\pi f_k (t-\tau)} \\ &\approx \sum_{k=1}^K s_k(t) e^{j2\pi f_k (t-\tau)} = \sum_{k=1}^K \tilde{s}_k(t) e^{-j2\pi f_k \tau} \end{aligned} \quad (2)$$

where $s_k(t)$, $\tilde{s}_k(t)$, $k = \{1, 2, \dots, K\}$ denote the k^{th} baseband signal and corresponding modulated signal with carrier frequency f_k , respectively. The reason of the approximation in (2) is the narrow-band assumption. We further make other assumptions similar to [11] on the above signal model:

- The baseband signals $\{s_k(t)\}_{k=1}^K$ are supposed to be mutually orthogonal and are bandlimited to $B_k = [-B_k/2, B_k/2]$, $k = \{1, 2, \dots, K\}$. We further assume that $\forall k = \{1, 2, \dots, K\}$, $B_k \leq B$.
- The MBS $x(t)$ is assumed to be bandlimited to $\mathcal{F} = [0, 1/T]$ and T denotes the Nyquist sampling interval of $x(t)$. We further assume that $1/T \gg B$, that is to say, the total bandwidth of signals is far less than the total spectrum range.
- Assume that the information bands do not overlap, i.e., $\{I(\hat{S}_i(f)) \cap I(\hat{S}_j(f)) = \emptyset : i, j \in \{1, 2, \dots, K\}\}$ where $\hat{S}_i(f)$ denotes the Fourier transform of modulated signal $s_i(t) e^{j2\pi f_i t}$ and $I(\hat{S}_i(f))$ represents the support region of $\hat{S}_i(f)$. This assumption satisfies that the carrier frequencies $\{f_i\}_{i=1}^K$ are distinct and corresponding signal spectral bands do not overlap.

B. Proposed Array Architecture

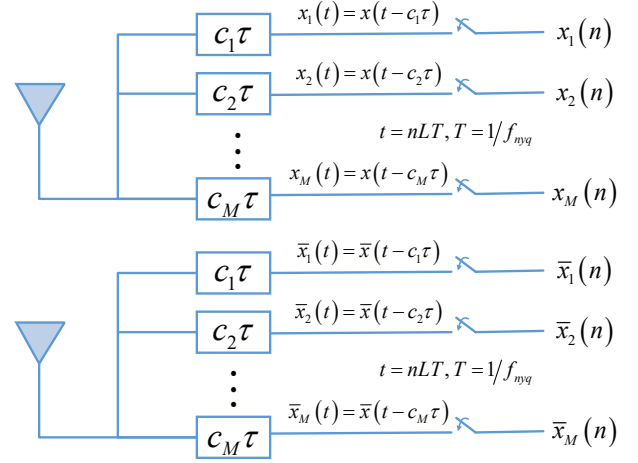


Fig. 1. Proposed Array Radar Structure (Binary Array)

Fig.1 depicts the receiving array radar structure proposed in this paper. This array structure has only two array elements, and the first one is considered as the reference element. The distance between the two elements is denoted as d , and d is equal to the half-wavelength of the signal whose frequency is the Nyquist sampling rate f_{Nyq} . Each array element connects separately to an identical multi-coset structure including M branches followed by samplers at LT sampling intervals, where L and T denote the sampling rate reduction factor and the Nyquist sampling interval, respectively. Denote the minimal delay unit as τ and the delay coefficients of these M channels are denoted as $C = [c_1, \dots, c_M]$, $0 = c_1 < \dots < c_M$. The delay pattern can be similarly set up to the array pattern of a sparse array, such as MRAs [8], coprime arrays.

We can express the output signal of the m^{th} path of the reference element as $x_m(t)$ and further define the signal model of the other array element as the form $\bar{(\cdot)}$. Therefore, the outputs of the m^{th} path of the reference element and the other one $x_m(t)$, $\bar{x}_m(t)$, can be expressed as

$$\begin{aligned} x_m(t) &= \sum_{k=1}^K \tilde{s}_k(t) e^{-j\omega_k c_m} + n_m(t) \\ \bar{x}_m(t) &= \sum_{k=1}^K \tilde{s}_k(t) e^{-j\omega_k c_m} e^{-j\phi_k} + \bar{n}_m(t) \end{aligned} \quad (3)$$

where $\omega_k \triangleq 2\pi f_k \tau$, $\phi_k \triangleq 2\pi d f_k \sin(\theta_k)/c$, and $n_m(t)$, $\bar{n}_m(t)$ are additive noise of corresponding paths. θ_k is the DOA of the k^{th} signal. ω_k is the unit phase difference caused by the delay unit, including only frequency information f_k ; ϕ_k is the unit phase difference derived from the array structure, including joint frequency and angle information $\{f_k, \theta_k\}$. Moreover, the additive noise of all channels obeys zero-mean Gaussian distribution with variance σ^2 and is statistically independent of signals.

Consider the received signals of all channels written as matrix form

$$\mathbf{x}_{all} = \begin{bmatrix} \mathbf{x}(t) \\ \bar{\mathbf{x}}(t) \end{bmatrix} = \begin{bmatrix} \mathbf{A}_t \\ \mathbf{A}_t \mathbf{D}_\phi \end{bmatrix} \mathbf{s}(t) + \begin{bmatrix} \mathbf{n}(t) \\ \bar{\mathbf{n}}(t) \end{bmatrix} \quad (4)$$

where $\mathbf{A}_t(\omega) = [\mathbf{a}_t(\omega_1) \cdots \mathbf{a}_t(\omega_K)]_{M \times K}$ is time-delay manifold matrix including only the frequency information, $\mathbf{D}_\phi = \text{diag}(e^{-j\phi_1}, \dots, e^{-j\phi_K})$ is a diagonal matrix including frequency and DOA information, and $\mathbf{n}(t), \bar{\mathbf{n}}(t)$ are the matrices of the noise, whose rows represent an additive noise of the different paths.

III. PROPOSED APPROACH

In this section, we put forward an approach to identify as many signals as possible at sub-Nyquist sampling in a binary array radar structure. This approach contains a joint estimation algorithm and an expansion method for increasing the number of identifiable signals.

A. Frequency Domain and Time Domain Analyses

According to [11], at sub-Nyquist structures, time domain data is typically converted to frequency domain data for analysis. Therefore, the discrete time Fourier transform of sampled signal of the m^{th} path at $f_s = f_{nyq}/L$ sampling rate can be expressed as

$$\begin{aligned} X_m(e^{j2\pi fT}) &= \sum_{k=1}^K e^{-j\omega_k c_m} S_k^p(f) + N_m^p(f) \\ \bar{X}_m(e^{j2\pi fT}) &= \sum_{k=1}^K e^{-j\omega_k c_m} e^{-j\phi_k} S_k^p(f) + \bar{N}_m^p(f) \end{aligned} \quad (5)$$

where $S_k^p(f) = \sum_{i \in \mathbb{Z}} \tilde{S}_k(f - if_s), k \in \{1, 2, \dots, K\}, f \in [0, f_{sub})$ denotes the aliased spectrum of k^{th} signal, and $N_m^p(f_s) = \sum_{i \in \mathbb{Z}} N_m(f - if_s), m \in \{1, 2, \dots, M\}$ represent the aliased noise spectrum. Thus, The spectral data of all channels can be reformulated as matrix form

$$\mathbf{X}_{all} = \begin{bmatrix} \mathbf{X}(f) \\ \bar{\mathbf{X}}(f) \end{bmatrix} = \begin{bmatrix} \mathbf{A}_t \\ \mathbf{A}_t \mathbf{D}_\phi \end{bmatrix} \mathbf{S}(f) + \begin{bmatrix} \mathbf{N}(f) \\ \bar{\mathbf{N}}(f) \end{bmatrix} \quad (6)$$

where $\mathbf{S}(f) = [S_1^p(f), S_2^p(f), \dots, S_K^p(f)]^T$ and $\mathbf{N}(f) = [N_1^p(f), N_2^p(f), \dots, N_M^p(f)]^T$. We form the following covariance matrix

$$\begin{aligned} \mathbf{R}_{X_{all}} &= E\{\mathbf{X}_{all} \mathbf{X}_{all}^H\} = \begin{bmatrix} \mathbf{R}_{XX} & \mathbf{R}_{X\bar{X}} \\ \mathbf{R}_{\bar{X}X} & \mathbf{R}_{\bar{X}\bar{X}} \end{bmatrix} \\ &= \begin{bmatrix} \mathbf{A}_t \\ \mathbf{A}_t \mathbf{D}_\phi \end{bmatrix} \mathbf{W} \begin{bmatrix} \mathbf{A}_t \\ \mathbf{A}_t \mathbf{D}_\phi \end{bmatrix}^H + L\sigma^2 \mathbf{I}_{2M} \\ &= \mathbf{A} \mathbf{W} \mathbf{A}^H + L\sigma^2 \mathbf{I}_{2M} \end{aligned} \quad (7)$$

where $\mathbf{A} = [\mathbf{a}(f_1, \phi_1), \mathbf{a}(f_2, \phi_2), \dots, \mathbf{a}(f_K, \phi_K)]$ and $\mathbf{a}(f_k, \phi_k)$ contains the information of frequency and corresponding DOA of the k^{th} signal; $\mathbf{W} = E\{\mathbf{S}(f) \mathbf{S}^H(f)\} = \text{diag}(W_1, \dots, W_K)$ and W_k denotes the k^{th} signal power. Notice that noise power goes up to $L\sigma^2$, because the noise power spectrum is folded under sub-Nyquist sampling.

B. Proposed Algorithm for Estimation of Carrier Frequency and DOAs

Due to the diagnose matrix \mathbf{D}_ϕ , we can exchange the positions of \mathbf{D}_ϕ and \mathbf{W} in the matrix block in (7), and the correlation matrix $\mathbf{R}_{X_{all}}$ becomes the following form

$$\mathbf{R}_{X_{all}} = \begin{bmatrix} \mathbf{A}_t \mathbf{W} \mathbf{A}_t^H & \mathbf{A}_t \mathbf{W} \mathbf{D}_\phi^H \mathbf{A}_t^H \\ \mathbf{A}_t \mathbf{W} \mathbf{D}_\phi \mathbf{A}_t^H & \mathbf{A}_t \mathbf{W} \mathbf{A}_t^H \end{bmatrix} + L\sigma^2 \mathbf{I}_{2M} \quad (8)$$

Notice that the two matrix blocks $\mathbf{R}_{XX}, \mathbf{R}_{\bar{X}\bar{X}}$ on the diagonal of the correlation matrix $\mathbf{R}_{X_{all}}$ in (8) have the same form i.e., $\mathbf{A}_t \mathbf{W} \mathbf{A}_t^H + L\sigma^2 \mathbf{I}_M$, which contains only frequency information. According to the MUSIC algorithm [13], Use eigen-decomposition on the matrix blocks to obtain corresponding matrices $\hat{\mathbf{G}}$ composed of eigenvectors corresponding to the noise subspace. The scanning function of pseudo spectrum can be written as follow

$$\hat{P}(\omega) = \frac{1}{\mathbf{a}_t^H(\omega) \hat{\mathbf{G}} \hat{\mathbf{G}}^H \mathbf{a}_t(\omega)} \quad (9)$$

As a result, use twice MUSIC algorithm on the two matrix blocks to obtain two Pseudo spectrums, and estimate carrier frequencies twice. Average two frequency estimations, and the final estimates of the frequencies $\{\hat{f}_k\}_{k=1}^K$ can be obtained.

According to (7), \mathbf{A} contains all information of frequencies and corresponding DOAs, which have been paired and cannot become ambiguous. Use eigen-decomposition on the correlation matrix $\mathbf{R}_{X_{all}}$ to obtain corresponding matrix $\hat{\mathbf{U}}$ composed of eigenvectors corresponding to the noise subspace. Utilize the following scanning function to obtain corresponding DOAs

$$\hat{P}(\hat{f}_k, \phi) = \frac{1}{\mathbf{a}^H(\hat{f}_k, \phi) \hat{\mathbf{U}} \hat{\mathbf{U}}^H \mathbf{a}(\hat{f}_k, \phi)} \quad (10)$$

where $k = \{1, 2, \dots, K\}$. Based on MUSIC algorithm, this scanning function (10) is combined with frequency estimation $\{\hat{f}_k\}_{k=1}^K$ to obtain the corresponding DOA estimation. This complete joint estimation algorithm is named after JDF4BA and its specific processing steps are as follows:

TABLE I
ALGORITHM JDF4BA

Step	Operation
1)	Calculate covariance matrix $\mathbf{R}_{X_{all}}$ according to (7);
2)	Eigen Decompose matrix blocks $\mathbf{R}_{XX}, \mathbf{R}_{\bar{X}\bar{X}}$ to get $\hat{\mathbf{G}}$;
3)	Use (9) to estimate the frequencies twice;
4)	Average the two frequency estimation to acquire a final frequency estimation $\{\hat{f}_k\}_{k=1}^K$;
5)	Eigen Decompose on $\mathbf{R}_{X_{all}}$ to obtain $\hat{\mathbf{U}}$;
6)	According to $\{\hat{f}_k\}_{k=1}^K$, orderly utilize (10) to get joint estimation $\{\hat{f}_k, \hat{\theta}_k\}_{k=1}^K$, notice $K < M$.

C. Expansion of Time-Delay Manifold

Since the JDF4BA algorithm utilizes the orthogonal characteristic between the noise subspace and the manifold vector, JDF4BA algorithm can estimate up to $M - 1$ signals. The

aim of this subsection is to achieve the breakthrough of the number of identifiable signals on such a binary array radar i.e., the more number of identifiable signals.

According to (8), we first make column vectorization on 4 matrix blocks of $\mathbf{R}_{X_{all}}$, and the outputs are expressed as

$$\begin{aligned}\mathbf{r}_{XX} &= \text{vec}(\mathbf{R}_{XX}) = (\mathbf{A}_t^* \odot \mathbf{A}_t) \mathbf{w} + L\sigma^2 \mathbf{i}_M \\ \mathbf{r}_{X\bar{X}} &= \text{vec}(\mathbf{R}_{X\bar{X}}) = (\mathbf{A}_t^* \odot \mathbf{A}_t) \mathbf{D}_\phi^* \mathbf{w} \\ \mathbf{r}_{\bar{X}X} &= \text{vec}(\mathbf{R}_{\bar{X}X}) = (\mathbf{A}_t^* \odot \mathbf{A}_t) \mathbf{D}_\phi \mathbf{w} \\ \mathbf{r}_{\bar{X}\bar{X}} &= \text{vec}(\mathbf{R}_{\bar{X}\bar{X}}) = (\mathbf{A}_t^* \odot \mathbf{A}_t) \mathbf{w} + L\sigma^2 \mathbf{i}_M\end{aligned}\quad (11)$$

where $\mathbf{w} = [W_1, \dots, W_K]^T$ and $\mathbf{i}_M = \text{vec}(\mathbf{I}_M)$. \odot , $\text{vec}(\cdot)$ represent Khatri-Rao product and column vectorization, respectively. The Khatri-Rao product of the manifold matrix is actually a virtual extension of the manifold matrix. Hence, design matrix transformation operator as Ξ to rearrange virtual manifold matrix and obtain the continuous manifold matrix \mathbf{A}_t^c , shown as follow

$$\mathbf{A}_t^c = \Xi(\mathbf{A}_t^* \odot \mathbf{A}_t) = [\mathbf{a}_t^c(\omega_1) \ \cdots \ \mathbf{a}_t^c(\omega_K)] \quad (12)$$

where $\mathbf{a}_t^c(\omega_k) = [e^{j\omega_k(Q-1)}, \dots, e^{-j\omega_k(Q-1)}]^T$. Q denotes the degree of freedom of expansion. Therefore, via matrix transformation operator, we can obtain

$$\begin{aligned}\mathbf{z}_{XX}^c &= \mathbf{A}_t^c \mathbf{w} + L\sigma^2 \Xi \mathbf{i}_M \\ \mathbf{z}_{X\bar{X}}^c &= \mathbf{A}_t^c \mathbf{D}_\phi^* \mathbf{w} \\ \mathbf{z}_{\bar{X}X}^c &= \mathbf{A}_t^c \mathbf{D}_\phi \mathbf{w} \\ \mathbf{z}_{\bar{X}\bar{X}}^c &= \mathbf{A}_t^c \mathbf{w} + L\sigma^2 \Xi \mathbf{i}_M\end{aligned}\quad (13)$$

According to [10], define the extraction matrix as $\Gamma_i = [\mathbf{0}_{Q \times (i-1)}, \mathbf{I}_Q, \mathbf{0}_{Q \times (Q-i)}]_{Q \times (2Q-1)}$, $i = \{1, 2, \dots, Q\}$ and carry out the following process

$$\begin{aligned}\mathbf{z}_{XX}^c &= \Gamma_i \mathbf{z}_{XX}^c \\ \mathbf{z}_{X\bar{X}}^c &= \Gamma_i \mathbf{z}_{X\bar{X}}^c \\ \mathbf{z}_{\bar{X}X}^c &= \Gamma_i \mathbf{z}_{\bar{X}X}^c \\ \mathbf{z}_{\bar{X}\bar{X}}^c &= \Gamma_i \mathbf{z}_{\bar{X}\bar{X}}^c\end{aligned}\quad (14)$$

Rearrange the above expressions and obtain new correlation matrix blocks as follows

$$\begin{aligned}\mathbf{R}_{XX}^v &= \begin{bmatrix} \mathbf{z}_{XXQ}^c & \cdots & \mathbf{z}_{XX1}^c \end{bmatrix} \\ &= \mathbf{A}_t^v \mathbf{W} (\mathbf{A}_t^v)^H + L\sigma^2 \mathbf{I}_Q \\ \mathbf{R}_{X\bar{X}}^v &= \begin{bmatrix} \mathbf{z}_{X\bar{X}Q}^c & \cdots & \mathbf{z}_{X\bar{X}1}^c \end{bmatrix} \\ &= \mathbf{A}_t^v \mathbf{W} \mathbf{D}_\phi^H (\mathbf{A}_t^v)^H \\ \mathbf{R}_{\bar{X}X}^v &= \begin{bmatrix} \mathbf{z}_{\bar{X}XQ}^c & \cdots & \mathbf{z}_{\bar{X}X1}^c \end{bmatrix} \\ &= \mathbf{A}_t^v \mathbf{W} \mathbf{D}_\phi (\mathbf{A}_t^v)^H \\ \mathbf{R}_{\bar{X}\bar{X}}^v &= \begin{bmatrix} \mathbf{z}_{\bar{X}\bar{X}Q}^c & \cdots & \mathbf{z}_{\bar{X}\bar{X}1}^c \end{bmatrix} \\ &= \mathbf{A}_t^v \mathbf{W} (\mathbf{A}_t^v)^H + L\sigma^2 \mathbf{I}_Q\end{aligned}\quad (15)$$

where $\mathbf{A}_t^v = [\mathbf{a}_t^v(\omega_1), \dots, \mathbf{a}_t^v(\omega_K)]$ denotes the virtual manifold matrix, and $\mathbf{a}_t^v(\omega_k) = [e^{-j\omega_k 0}, \dots, e^{-j\omega_k(Q-1)}]$ represents the virtual manifold vector. Collect the above correlation matrix blocks and form a new correlation matrix

$$\mathbf{R}_{X_{all}}^v = \begin{bmatrix} \mathbf{A}_t^v \mathbf{W} (\mathbf{A}_t^v)^H & \mathbf{A}_t^v \mathbf{W} \mathbf{D}_\phi^H (\mathbf{A}_t^v)^H \\ \mathbf{A}_t^v \mathbf{W} \mathbf{D}_\phi (\mathbf{A}_t^v)^H & \mathbf{A}_t^v \mathbf{W} (\mathbf{A}_t^v)^H \end{bmatrix} + L\sigma^2 \mathbf{I}_{2Q} \quad (16)$$

It can be seen that the structure of the new correlation matrix is actually similar to that of the correlation matrix $\mathbf{R}_{X_{all}}$ in (8), and frequencies and DOAs in the new manifold matrix have been already matched up, and the dimension of the correlation matrix increases from M to Q . Thus, we can use JDF4BA algorithm on these new correlation matrix $\mathbf{R}_{X_{all}}^v$ to identify $Q-1$ signals, and this expansion of time-delay manifold method is named after ETM method. The specific steps for JDF4BA algorithm combined with ETM method to identify signals is shown in TABLE II below

TABLE II
ALGORITHM JDF4BA WITH ETM

Step	Operation
1)	Calculate covariance matrix $\mathbf{R}_{X_{all}}$ according to (7);
2)	Make column vectorization on matrix blocks of $\mathbf{R}_{X_{all}}$ according to (11);
3)	Utilize (12) to select the continuous manifold matrix and obtain (13);
4)	Use extraction Γ_i and rearrange vectors according to (15);
5)	Collect the new matrix blocks to obtain new correlation matrix $\mathbf{R}_{X_{all}}^v$ according to (16);
6)	Use algorithm JDF4BA on new correlation matrix $\mathbf{R}_{X_{all}}^v$ to get joint estimation $\{\hat{f}_k, \hat{\theta}_k\}_{k=1}^K$, notice $K < Q$.

D. Analyses of sampling rate reduction factor and the number of identifiable signals

With the proposed method on the binary array, the joint estimation technique is effective if

- i. $Q \geq K + 1$
- ii. $L \leq 1/BT$.

The algorithm JDF4BA based on MUSIC algorithm can estimate the carrier frequencies and corresponding DOAs of MBS signal, by utilizing the noise subspace. Therefore, the dimension Q of expansion of time-delay manifold has to be larger than the number K of signals. For the second condition, due to assumptions from II-A, f_s should satisfy that the periodic spectrums i.e., $S_k^p(f) = \sum_{i \in \mathbb{Z}} \tilde{S}_k(f - if_s)$, $k \in \{1, 2, \dots, K\}$, $f \in [0, f_{nyq}]$ do not alias. This is possible if $f_s \geq B$ or $L \leq 1/BT$, the maximum bandwidth is assumed to be B according to the assumption.

IV. SIMULATION

In this section, numerical simulations are conducted to confirm the validity and performance of the proposed approach. According to [16], the MRA has the maximum virtual aperture in the condition of the same array element among the sparse arrays; therefore, the delay pattern we set up

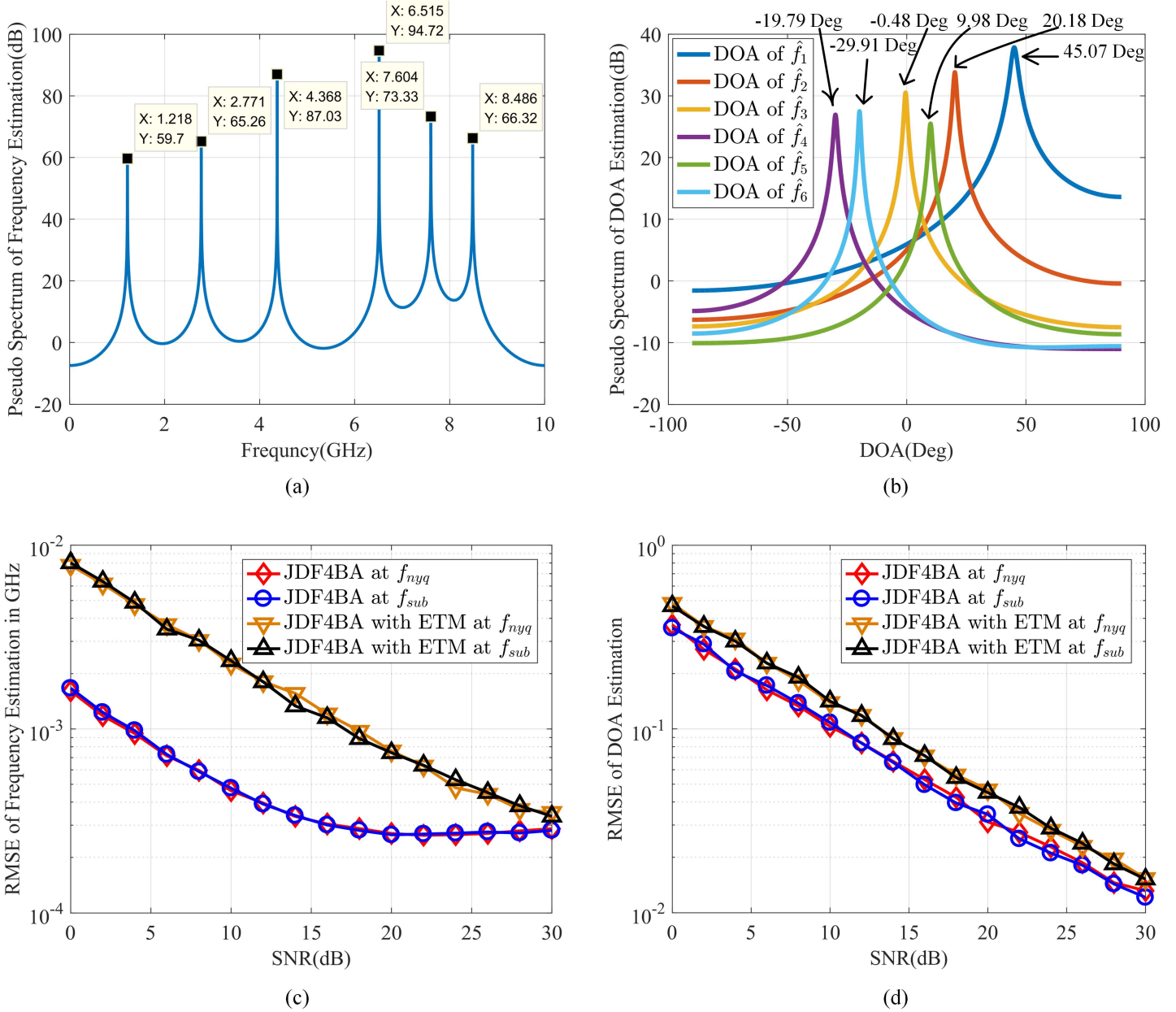


Fig. 2. Pseudo spectrum via algorithm JDF4BA with ETM (the bandwidth of each signal $B = 25\text{MHz}$, $\text{SNR} = 10\text{dB}$, and the sub-Nyquist sampling rate $f_{sub} = 25\text{MHz}$, i.e., the sampling rate reduction factor $L = 400$): (a) Pseudo spectrum of frequency estimation according to (9); (b) Pseudo spectrum of DOA estimation (10). Performance comparison (all are complex-valued sinusoid signals, the Nyquist sampling rate $f_{nyq} = 10\text{GHz}$, and the sub-Nyquist sampling rate $f_{sub} = 100\text{MHz}$, i.e., the sampling rate reduction factor $L = 100$): (c) Frequency estimation performance comparison; (d) DOA estimation performance comparison.

$C = [c_1, \dots, c_M]$, $0 = c_1 < \dots < c_M$ is similar to the array element position of MRA. In our simulation we choose the Nyquist sampling rate $f_{nyq} = 1/T = 10\text{GHz}$, the minimal delay unit $\tau = T$, the number of paths following each array element $M = 4$, and the delay pattern $C = [0, 1, 4, 6]$. Hence, the path number of virtual time-delay channels of delay pattern C i.e., the dimension of expansion, is $Q = 7$. The Root Mean Square Error (RMSE) of parameters is defined as $\text{RMSE} = \sqrt{\frac{1}{N_m K} \sum_{i=1}^{N_m} \sum_{k=1}^K (u_k^i - \hat{u}_k^i)^2}$ where the super-

script i refers to the i^{th} trail, and N_m denotes the number of Monte Carlo tests. u_k^i and \hat{u}_k^i are the true parameter and estimated parameter in the i^{th} trail, respectively. The Signal to Noise Ratio (SNR) is defined as $\text{SNR} = (E(|x_m(t)|^2)/\sigma^2)$.

In the first simulation, the aim is to verify whether the algorithm JDF4BA with ETM method is valid and whether the conclusion of III-D is correct. We set up 6 QPSK signals of which the maximum information bandwidth inside is $B = 25\text{MHz}$ with following different carrier frequencies (in GHz) $\{1.22, 2.77, 4.32, 6.54, 7.64, 8.48\}$ and corre-

sponding DOAs (in degrees) $\{45, 20, 0, -30, 10, -20\}$. We choose the sub-Nyquist sampling rate $f_{sub} = 25\text{MHz}$, same as the maximum information bandwidth B , corresponding to sampling rate reduction factor $L = 400$. As shown in Fig.2 (a), according to the (9), the pseudo spectrum of frequency has 6 peaks so that we can obtain frequency estimation of signals. Seeing Fig. 2 (b), we then use (10) to get 6 pseudo spectrums of DOA, combined with $\{\hat{f}_k\}_{k=1}^K$. Finally, we can obtain $\{\hat{f}_k, \hat{\theta}_k\}_{k=1}^K$. According to simulation settings, the total sampling rate $f_{sub}^{total} = 2M \cdot f_{sub} = 200\text{MHz}$ is less than the total Nyquist sampling rate $f_{nyq}^{total} = 2M \cdot f_{nyq} = 80\text{GHz}$.

The second numerical simulation is to test the performance of algorithm JDF4BA with ETM method with different SNRs. We set up 6 complex sinusoid signals with following carrier frequencies $\{1.22, 2.77, 4.32, 6.54, 7.64, 8.48\}$ and corresponding DOAs $\{10, 20, 30, 30, 50, 80\}$. We choose the sub-Nyquist sampling rate $f_{sub} = 250\text{MHz}$, corresponding to sampling rate reduction factor $L = 40$. The number of Monte Carlo is 200. The conditions for comparison are the algorithm JDF4BA with ETM method at the Nyquist sampling rate, and the algorithm JDF4BA without ETM method at the sub-Nyquist sampling rate as well as the Nyquist sampling rate. Due to algorithm JDF4BA without ETM method, the number of identifiable signals is $M - 1 = 3$. Therefore, in the numerical simulation of the algorithm without ETM method, the signals we set up is the first three signals in set $\{f_k, \theta_k\}_{k=1}^K$.

As shown Fig.2 (c) (d), we can see the performance of frequencies and DOAs via JDF4BA with ETM is not as good as the performance of only JDF4BA under the same sampling rate. The reason is that ETM method is in exchange for slight sacrificing performance to be able to identify more signals. Moreover, only if the sub-Nyquist sampling rate f_{sub} is larger than the maximum bandwidth B , the performance is almost identical to that at the Nyquist sampling rate, because the information bands of signals are complete at sub-Nyquist sampling. Therefore, the performance is not related with the sampling rate if the sampling rate is larger than the maximum bandwidth.

V. CONCLUSION

In this paper, we put forward a binary array radar structure (each array element has M branches) and a novel approach (algorithm JDF4BA and ETM method) to jointly estimate frequencies and corresponding DOAs at sub-Nyquist sampling. Algorithm JDF4BA can achieve auto-pairing between frequencies and corresponding DOAs under the sub-Nyquist sampling rate $f_s \geq B$, thus avoiding ambiguity. Furthermore, ETM method increases the number of identifiable signals from $M - 1$ to $Q - 1$. As a consequence, the binary array radar structure with this approach just needs $2M$ paths to estimate $Q - 1$ signals with the total sampling rate $f_{sub}^{total} = 2MB$, which means fewer number of array elements (only 2), fewer number of channels, and smaller total sampling rate under the same number of signals, compared with the previous works.

Simulation results validate the effectiveness and performance of the present approach.

ACKNOWLEDGMENT

This work was supported by the Fundamental Research Funds for the Central Universities (Grant No. ZYGX2016Z005, and ZYGX2016J218).

REFERENCES

- [1] M. Unser, "Sampling-50 years after Shannon," *Proceedings of the IEEE*, vol. 88, no. 4, pp. 569–587, April 2000.
- [2] Y. C. Eldar, *Sampling Theory: Beyond Bandlimited Systems*. Cambridge University Press, 2014.
- [3] A. N. Lemma, A. van der Veen, and E. F. Deprettere, "Analysis of joint angle-frequency estimation using esprit," *IEEE Transactions on Signal Processing*, vol. 51, no. 5, pp. 1264–1283, May 2003.
- [4] X. Wang, X. Zhang, J. Li, and J. Bai, "Improved esprit method for joint direction-of-arrival and frequency estimation using multiple-delay output," *International Journal of Antennas & Propagation*, vol. 2012, no. 1, pp. 1018–1020, 2012.
- [5] M. D. Zoltowski and C. P. Mathews, "Real-time frequency and 2-d angle estimation with sub-nyquist spatio-temporal sampling," *IEEE Transactions on Signal Processing*, vol. 42, no. 10, pp. 2781–2794, Oct 1994.
- [6] D. D. Ariananda and G. Leus, "Compressive joint angular-frequency power spectrum estimation," in *Signal Processing Conference*, 2014, pp. 1–5.
- [7] M. Mishali and Y. C. Eldar, "Blind multiband signal reconstruction: Compressed sensing for analog signals," *IEEE Transactions on Signal Processing*, vol. 57, no. 3, pp. 993–1009, March 2009.
- [8] A. Moffet, "Minimum-redundancy linear arrays," *IEEE Transactions on Antennas & Propagation*, vol. 16, no. 2, pp. 172–175, 2003.
- [9] L. Liu and P. Wei, "Joint doa and frequency estimation with sub-nyquist sampling for more sources than sensors," *IET Radar, Sonar Navigation*, vol. 11, no. 12, pp. 1798–1801, 2017.
- [10] L. Liu and P. Wei, "Joint doa and frequency estimation with sub-nyquist sampling in the sparse array system," *IEEE Signal Processing Letters*, vol. 25, no. 9, pp. 1285–1289, Sept 2018.
- [11] A. A. Kumar, S. G. Razul, and C. S. See, "An efficient sub-nyquist receiver architecture for spectrum blind reconstruction and direction of arrival estimation," in *2014 IEEE International Conference on Acoustics, Speech and Signal Processing (ICASSP)*, May 2014, pp. 6781–6785.
- [12] A. A. Kumar, S. G. Razul, and C. S. See, "Carrier frequency and direction of arrival estimation with nested sub-nyquist sensor array receiver," in *2015 23rd European Signal Processing Conference (EUSIPCO)*, Aug 2015, pp. 1167–1171.
- [13] R. Schmidt, "Multiple emitter location and signal parameter estimation," *IEEE Transactions on Antennas and Propagation*, vol. 34, no. 3, pp. 276–280, March 1986.
- [14] R. Roy, A. Paulraj, and T. Kailath, "Esprit—a subspace rotation approach to estimation of parameters of cisoids in noise," *IEEE Transactions on Acoustics, Speech, and Signal Processing*, vol. 34, no. 5, pp. 1340–1342, October 1986.
- [15] J. B. Kruskal, "Three-way arrays: rank and uniqueness of trilinear decompositions, with application to arithmetic complexity and statistics," *Linear Algebra & Its Applications*, vol. 18, no. 2, pp. 95–138, 1977.
- [16] M. Wang and A. Nehorai, "Coarrays, music, and the cramrø bound," *IEEE Transactions on Signal Processing*, vol. 65, no. 4, pp. 933–946, Feb 2017.